Turning off low and high currents in a transmitter loop used in the transient electromagnetic method

Nikolai O. Kozhevnikov[1]*, Maxim V. Sharlov[2] and Sergei M. Stefanenko[1]

[1]*Institute of Petroleum Geology and Geophysics, Siberian Branch of the Russian Academy of Sciences, 3, prosp. Koptyuga, Novosibirsk 630090, Russia, and* [2]*SIGMA-GEO LLC, 6, Zvezdinskaya st., Irkutsk 664039, Russia*

ABSTRACT

In near-surface transient electromagnetic studies, it is desirable to measure the transient response starting from the earliest possible time. This requires the current in the transmitter loop to be switched off quickly, which necessitates working with a low transmitter current. As for deep-target transient electromagnetic studies, the transmitter current is as high as possible. The transmitter current's turn-off waveform and total duration affect the transient voltage response, especially at early times, which is to be accounted for when interpreting transient electromagnetic data. This article discusses the difference in switching off low and high current in a horizontal loop used as the source of the primary magnetic field in the transient electromagnetic method. Low and high currents are turned off in fundamentally different ways. When the current to be switched off is low, the loop can be represented as a symmetric combination of two transmission lines grounded at the middle of the loop perimeter. Such a representation of a loop allows calculating the current turn-off waveform at any point of the loop. The waveform and total duration of switching off a low current does not depend on its magnitude, but is determined by the period of natural oscillations of the current in the loop and the resistance of a shunting resistor. Switching off a low current in a loop can be represented as the sum of stepped current waves travelling along the loop wire. As a consequence, the current at different points of the loop perimeter is turned off at different times. In contrast to a low current, a high current is switched off linearly in time and synchronously at all points of the loop perimeter. The wave phenomena appear only at the very beginning of the current shutdown for a time interval that is much less than the total current turn-off duration. Presentation of the loop using a simple lumped-circuit model predicts the waveform and duration of the high current turn-off that coincide with the measured ones. There are two reasons why the article may be of interest to those engaged in the theory and/or practice of electromagnetic geophysical methods. First, it contributes to a general understanding of how the current in the transmitter loop is turned off. Second, the article shows how the parameters of a transmitter loop determine the current turn-off duration and thus the minimum depth of the transient electromagnetic sounding method.

Key words: Electromagnetics, Modelling.

1 INTRODUCTION

In the transient electromagnetic (TEM) sounding method, a horizontal wire loop is usually used to produce the primary

*E-mail: kno48@yandex.ru

magnetic field. The duration (t_{off}) and waveform of the transmitter current turn-off affects the early-time TEM response. According to Christiansen, Auken and Viezzoli (2011), the duration of current turn-off affects the transient response for two reasons. First, the induction currents in the earth depend on the duration of the transmitter current shutdown. Second, the time interval between the end of the transmitter current shutdown and of the earliest measurement time changes depending on the duration of the current shutdown. Most often, when accounting for these effects, one assumes that the transmitter current is turned off linearly with time (Sokolov, Tabarovsky and Rabinovich 1978; Raiche 1984; Asten 1987; Fitterman and Anderson 1987; Christiansen *et al.* 2011). In geophysical literature, transmitter and receiver loops are usually represented as an equivalent lumped circuit (Vishnyakov and Vishnyakova 1974; Zakharkin 1981; Fu, Zhou and Tai 2007; Schamper, Auken and Sørensen 2014; Wang *et al.* 2016; Sternberg, Dvorak and Feng 2017; Liu *et al.* 2019). Individual elements of lumped systems are thought of being concentrated at singular points in space. So the dependent variables of interest depend only on time. In general, this will mean solving a set of ordinary differential equations. A classic example is an electrical circuit having passive elements such as resistor, inductor and capacitor.

To induce transient eddy currents in the ground, a transmitter unit generates in the loop rectangular current pulses separated by pauses. In order to protect electronic switches from overvoltage, a transient voltage suppressor (TVS) device is connected in parallel to the loop, limiting, or clamping, the voltage across the loop (Ferreira *et al.* 2004; Zhao *et al.* 2013; Zhang *et al.* 2014).

Typically, the clamping voltage (V_c) is in the order of hundreds of volts or more. On the one hand, constant voltage clamping protects electronic switches from irreversible breakdown, on the other hand, it increases the duration of the transmitter current turn-off, the earliest measurement time and, accordingly, the minimum TEM sounding depth. Because of this, in near-surface TEM studies, the earliest part of the TEM response is measured at low transmitter current. In this case, the amplitude of the voltage surge across the loop terminals does not exceed V_c, and the loop exhibits properties characteristic of a distributed system (Kozhevnikov 2016). Unlike lumped systems, distributed systems are built based on the assumption of being distributed in space. Therefore, the physical quantities depend both on time and on space. In this case, we will be solving partial differential equations.

In this regard, it is interesting to compare turn-offs of high and low current in the transmitter loop. In this paper,

we first present experimental data illustrating how a large current is turned off in a 300 m by 300 m loop. Then, we show that presentation of the loop as an equivalent lumped circuit accounts for the measured high current turn-offs. After this, we discuss high and low current turn-off waveforms measured at different points of the 500 m by 500 m loop perimeter. Next, we consider the representation of a loop as a symmetric combination of two transmission lines and show that such a model explains the low current turn-offs. In conclusion, we discuss and give a summary of the main results of our research.

2 INSTRUMENTATION AND METHODS

Measurements the results of which are presented and discussed in the article, were performed using FastSnap equipment (Sharlov *et al.* 2017a; http://fastsnap.com.au/) consisting of the transmitter and receiver units. The transmitter unit is essentially a full-bridge converter, consisting of insulated-gate bipolar transistors and a constant voltage-clamping circuit. The transmitter unit is powered from a battery and generates bipolar rectangular current pulses separated by pauses. Depending on the transient electromagnetic (TEM) response decay rate, the duration of the pulses and pauses is 20 to 1000 milliseconds; the amplitude (I_0) of current pulses ranges from fractions of an ampere to 30 amperes. In the case of purely resistive load, the current turn-off time does not exceed 0.6 μs. The FastSnap transmitter unit clamps the voltage across the loop at about 500 volts with 1.5KE avalanche Transil diodes, the instantaneous response of which makes them particularly suited to protect voltage-sensitive devices.

The receiver unit records the TEM voltage response at a sampling interval of 25 ns to 205 μs.

The transient electromotive force (EMF) induced in the receiving loop is fed to the input of the amplifier with a gain from 1 to 280. The output voltage of the amplifier is digitized by 14-bit or 24-bit analog-to-digital converter (ADC) (depending on sampling rate). The maximum number of samples in one record is 14,000. Each record is saved in the long-term memory of the computer, which enables further digital processing of the TEM data.

The TEM response curve is measured in separate overlapping segments with parameters optimized for each stage of the TEM response. At early times, the measurement is carried out at low transmitter current, small gain and high sampling frequency. The later segments of the TEM voltage response are recorded at a higher transmitter current and/or a larger gain, and a lower sampling frequency. Each portion of the TEM signal is recorded repeatedly, after which the individual

records are stacked. When measuring later parts of the TEM response, the number of individual records increases. At the final stage, all segments are combined into the resulting TEM voltage response curve. Usually, the number of segments is in the range of 5–10.

To further enhance S/N ratio, digital filtering procedures can be used at different stages of the signal processing. Raw time-series data can be filtered before averaging, while averaged data can be filtered afterwards with other settings. Before the assembly of separate records into a final TEM voltage curve, linear sampling is interpolated to the logarithmic scale. Filtering is not mandatory and is applied only when necessary to remove noise of specific types. In most cases, the full dynamic range of the final voltage response is about 140 dB, which allows measuring the voltage ranging from several volts to about one tenth of a microvolt.

The transmitter and receiver units are connected to a control PC (a laptop) via a digital communication line adapter and transmission lines that may reach 400 m long. The transmitter and receiver units are synchronized internally (GPS antenna) or externally (cables). The transmitter is managed either manually by a built-in control panel or automatically by a program run on the control PC. A built-in GPS indicates longitude, latitude and altitude.

To study the current turn-off, we used the FastSnap measuring unit as a precise digital oscilloscope to record the voltage across a shunt resistor that was connected serially with the loop wire. The current was calculated as $V(t)/R_{sh}$. To estimate the retardation (lag) in the current turn-off, we placed the shunt resistor at various points on the loop perimeter P. If we take one of the loop terminals as the reference point, and the distance from this terminal along the wire as the x coordinate, the x coordinate of the other terminal corresponds to P. Usually, the current turn-off was recorded at $x = 0$, $P/4$, and $P/2$. Figure 1(a) illustrates the general measurement set-up, and Fig. 1(b) shows the shunt resistor placed in the central point of the loop perimeter ($x = P/2$).

## 3 HIGH CURRENT SWITCH-OFF AND EQUIVALENT LUMPED-CIRCUIT MODEL

Figure 2 shows the measured turn-off waveforms of a high current in a 300 m by 300 m loop. The measurements were carried out in the spring of 2017 on the ice cover of Lake Baikal as a part of an experiment to study the intrinsic transient response of the FastSnap measuring system (Sharlov, Kozhevnikov and Sharlov 2017b). A current shunt with resistance $R_{sh} = 0.003$ ohm was placed at the midpoint of the loop
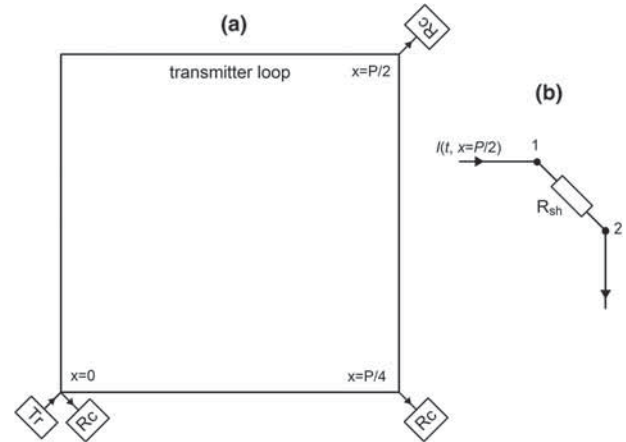

Figure 1 Field set-up for measuring current's turn-off in a loop: (a) general view; (b) a shunt resistor placed in the middle point of the loop perimeter. FastSnap units: Tr, transmitter; Rc, receiver. Receiver unit records the voltage $V(t)$ across points 1 and 2, after which the current $I(t)$ is calculated as $V(t)/R$sh.

perimeter. As evident from Fig. 2, the current decays linearly with time; only at the earliest times one can see some retardation effects which, as we show in this paper, are due to the fact that a loop is essentially a distributed circuit.

Figure 3 displays the plot of current turn-off duration versus the amplitude of current pulses in the 300 m by 300 m transmitter loop. Small crosses indicate the measured data, the solid line is the calculated regression line, and the dotted line is the extrapolation of the regression line to the region of
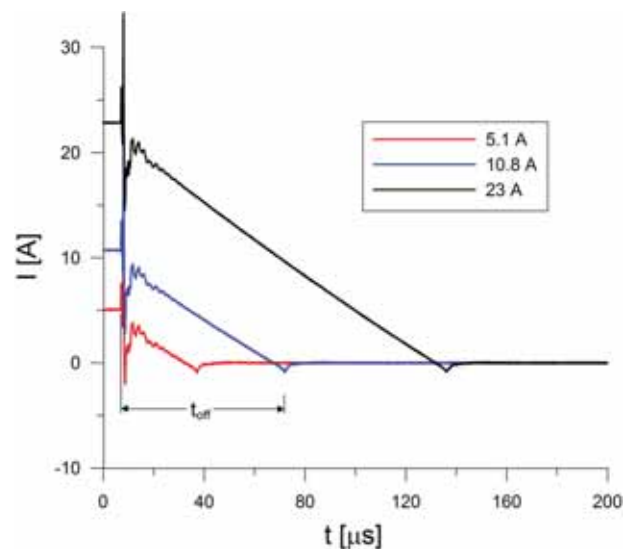
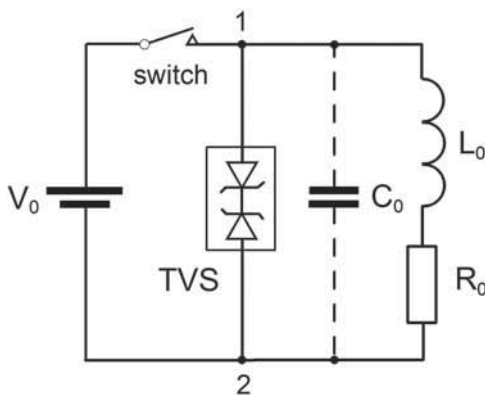**Figure 2** High current turn-offs in the 300 m by 300 m transmitter loop.
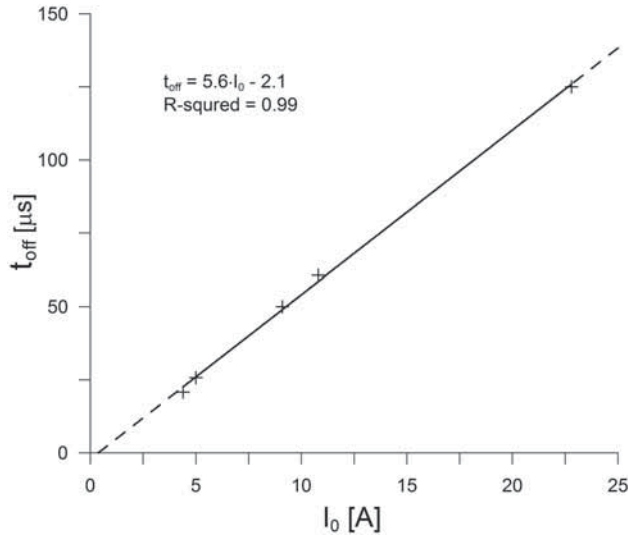
Figure 3 Relationship between the current pulse amplitude (I_0) and duration of the current turn-off (t_{off}) for the 300 m by 300 m transmitter loop. Small crosses represent the experimental data. The solid line is the linear regression plot; its extrapolation to the region of high and low currents is shown as a dashed line.

higher ($I_0 > 23$ A) and lower ($I_0 < 5$ A) currents. According to Fig. 3, the current turn-off duration (in μs) in the 300 m by 300 m transmitter loop can be estimated using the formula:

$$t_{off} = 5.6\, I_0. \tag{1}$$

In Fig. 4, the transmitter loop is represented as an equivalent circuit with lumped inductance L_0, capacitance C_0 and resistance R_0. The battery and the switch are connected in se-

Figure 4 Presentation of the transmitter loop as an equivalent lumped circuit. The voltage source and the switch are connected in series with the loop. To limit the surge voltage induced across the loop during the current turn-off, the loop is shunted by a transient voltage suppressor (TVS) device.

ries with the circuit. Upon closing the switch, after some time the steady current $I_0 = V_0/R_0$ will flow through the loop. At the instant the switch is opened, a voltage surge arises across the loop terminals (points 1 and 2 in Fig. 4). If its amplitude, V_{max}, does not exceed the switch failure, or irreversible breakdown voltage V_{bd} (such as one at which the switch is damaged), then (Ott 2009, p. 320)

$$V_{max} = I_0\sqrt{L_0/C_0}. \tag{2}$$

When the transmitter current is high and/or the loop inductance is large, V_{max} can exceed V_{bd}, and the failure of the switch will occur. As mentioned above, the loop is usually shunted by a TVS device clamping the voltage across the loop at the constant value $V_c < V_{bd}$ and thus protecting the switch from the failure. In this case, the voltage across the loop very quickly rises to V_c, after which it remains equal to V_c until the current is turned off. Since during this time the loop capacitance C_0 is shunted by very low dynamic resistance of the TVS device, the current switching-off obeys the equation:

$$L_0\frac{dI}{dt} + I R_0 = V_c. \tag{3}$$

Since usually $L_0(dI/dt) >> IR_0$,

$$L_0\frac{dI}{dt} = V_c, \tag{4}$$

whence it follows that

$$\frac{dI}{dt} = \frac{V_c}{L_0}. \tag{5}$$

Thus, the current's decay rate is constant and equal to V_c/L_0, which means that the current turns off linearly with time. Because of this, (5) can be written as

$$\frac{I_0}{t_{off}} = \frac{V_c}{L_0}, \tag{6}$$

whence

$$t_{off} = I_0\frac{L_0}{V_c}. \tag{7}$$

The inductance of the 300 m by 300 m loop, measured by an LCR meter, is 2.86 mH. Substituting in (7) $V_c = 500$ volts, and $L_0 = 2.86 \times 10^{-3}$H for different I_0 values indicates that calculated turn-off durations differ, on the average, from the measured ones by about 8.5%. This means that an equivalent lumped circuit reasonably accounts for turning off high current in the transmitter loop.

4 HOW LOW AND HIGH CURRENT
   TURN-OFFS DIFFER

In near-surface transient electromagnetic (TEM) studies, it is desirable to take measurements starting from the earliest possible time, which entails the need to work with a low current in the transmitter loop. In this case, the voltage surge across the loop does not reach V_c, and the current switch-off differs from that considered above.

The distinction between the switching off of low and high currents is illustrated by the current turn-off waveforms measured at different points of the 500 m by 500 m loop perimeter. The measurements were carried out in the Olkhon region on the western shore of Lake Baikal. Current turn-off waveforms were studied by recording the voltage across a 0.075 ohm shunt resistor connected serially with the loop wire at $x = 0$, $P/4$, and $P/2$. Disconnecting the loop from the battery may result in high-frequency current oscillation (oscillation mode). Because of this, the loop is usually shunted by a resistor the resistance of which enables optimal oscillation damping (matching mode). In the case under consideration, the loop was shunted by a 500 ohm resistor. Figure 5 displays turn-off waveforms for low (0.75 A) and high (9 A) currents. The current turn-off waveforms and the total current turn-off durations for high and low currents are fundamentally different.

The low current turn-off waveforms bear no resemblance to a ramp function and depend on the location of the measuring current shunt. Not counting some 'second-order' features, the waveforms of low current's turn-off can be represented as a sum of delayed step functions. This is especially evident in Fig. 5(b), where both time and current scales are adjusted to show the details of the low current turn-off. Although the turn-off waveforms differ depending on the position of the measurement point along the loop perimeter, one can determine the total off time as such after that the current becomes close to zero at all points of the loop perimeter.

As for the high current (see Fig. 5a), by and large it decreases linearly and synchronously with time at all points of the loop perimeter; delay effects are noticeable only at the beginning of the current shutdown. The time interval during which the delay is observed is about 15 μs, while the total duration of the current shutdown is about 100 μs. Because of this, it is reasonable to assume that once the current is switched off, the after-effect of the retardation does not contribute significantly to the overall TEM response.
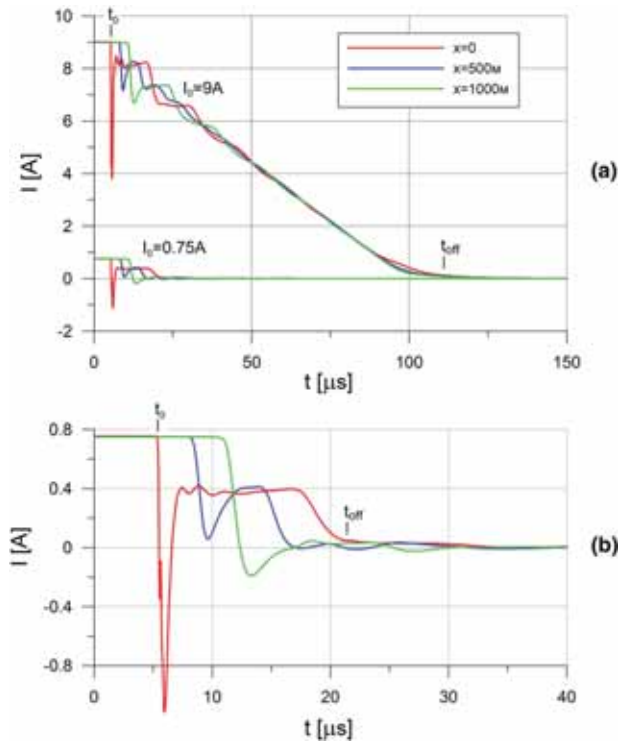

Figure 5 Current turn-off waveforms recorded at different points of the 500 m by 500 m loop perimeter. (a) High (9 A) and low (0.75 A) current turn-offs. (b) Detailed picture of the low current switching off. At t_0, the transmitter disconnects the loop from the battery.

Figure 6 shows low and high current turn-off waveforms for the midpoint of the loop perimeter ($x = 1000$ m). As it is easy to see, turning off a large current involves two stages. First, during the time interval from t_0 to about 25 μs, delay effects are observed. Over this interval, which equals the turn-off time of the small current, the high current decreases from 9 A to 7.35 A, and the time dependence of the high current decay is exactly the same as of the low current. At $t > 25$ μs, the high current is switched off linearly.

Along with experimental current turn-off waveforms, Fig. 6 displays the calculated regression line for the high current turn-off over the time interval from t_0 to 100 μs (coefficient of determination $R^2 = 0.99$). As estimated from the linear fitting plot, the total turn-off time is about 95 μs. The inductance of the 500 m by 500 m loop measured with an LCR meter is 5 mH. Substitution in (7) $V_c = 500$ volts, $L = 5 \times 10^{-3}$ H, $I_0 = 9$ A gives $t_{off} = 90$ μs, which agrees well with the measurement (see Fig. 5a) and linear fitting results and indicates, once again, that in simulating the shutdown of the high current the loop can be considered as a circuit with lumped elements.
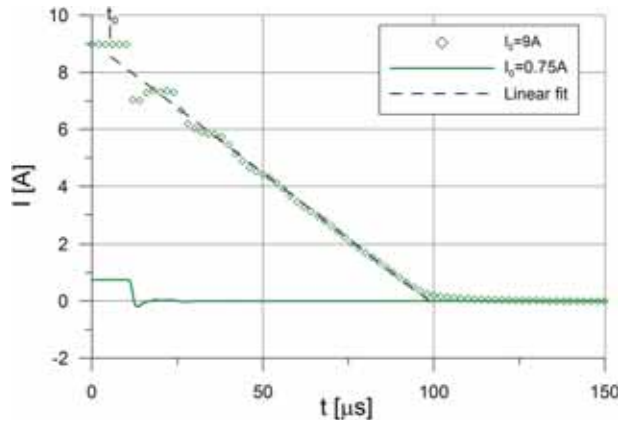
Figure 6 Low and high current turn-off waveforms for the midpoint of the loop perimeter ($x = 1000$ m) and a linear graph fitting the high current turn-off over the time interval from t_0 to 100 μs (coefficient of determination $R^2 = 0.99$).

Figure 7 demonstrates switch-off waveforms of the 0.2 A (top) and 0.75 A (bottom) currents for $x = 0$, 500 and 1000 m. The dot marks the instant when the loop is disconnected from the battery. It can be seen that for fixed x, turn-off waveforms of 0.2 A and 0.75 A current are similar.

In Fig. 8, the solid line shows the 0.2 A current turn-off waveform, and the small crosses show the turn-off waveform of the 0.75 A current. When plotting graphs for the 0.2 A current, the current values were multiplied by $3.75 = 0.75$ A/0.2 A, so that the graphs for both currents are shown at the same vertical scale. In this case, it is clearly seen that the turn-off waveforms of the 0.2A current are identical to those of the 0.75 A current. Thus, if the transmitter current does not exceed that at which the voltage surge across the loop reaches V_c, the shape and duration of the turn-off do not depend on the current magnitude.

5 TRANSMISSION LINE MODEL

The above presentation of the loop as an equivalent lumped circuit (see Fig. 4) does not explain switching off a low current. Recall that when a low current is turned off, the amplitude of the voltage surge across the loop is less than V_c; therefore, the clamping device does not affect the current shutdown. Experimental data have indicated that in this case the loop exhibits properties typical of a transmission line (Kozhevnikov and Nikiforov 1998; Kozhevnikov and Nikiforov 2000; Helwig and Kozhevnikov 2003; Kozhevnikov 2006, 2009). These data can be summarized as follows:

1. The input impedance of a loop depends on frequency in the same way as the input impedance of a transmission line shorted at the output.
2. In an open loop, switch-off gives rise to standing current and voltage waves.
3. When the loop is shunted by a resistor with a resistance that minimizes high-frequency current oscillations (matching mode), one can clearly see a delay, or retardation in the stepwise current turn-off relative to the time instant of disconnecting the loop from the battery.

It may seem that a transmission line has little in common with a transmitter loop. However, due to its symmetry, the loop can be represented by a combination of two identical transmission lines. The lines are formed by the loop wire and the underlying ground and are grounded at the point where the lines' outputs meet. The current or voltage source can also be represented as a combination of two identical sources with the common point grounded.

Figure 9(a) shows a square loop, a battery with the voltage V_0 and a switch. The length of the wire forming the loop is equal to P. When the switch is closed, the steady current (I_0) flows in the loop. A matching resistor, R_1, is connected across the loop. At time $t = 0$, the switch opens, and the current supplied from the battery becomes zero.

In Fig. 9(b), the same loop is shown as a combination of two transmission lines. A battery with voltage $V_0/2$, a resistor with resistance $R_1/2$ and a switch are connected to the input of each line. At $t = 0$, each switch disconnects 'its] line from 'its' battery. Since, due to the symmetry of the loop, points O and $P/2$ have the same potential, they can be grounded, which would not affect the voltage and current distribution along the loop. Therefore, the calculation of switching off the current in the loop can be reduced to the calculation of the current turn-off in a transmission line having length of $l = P/2$ and shorted at its output (Fig. 9c).

Unlike the lumped circuit, the transmission line is described by *distributed* (per-unit-length) parameters, namely, resistance (R), inductance (L), capacitance (C) and insulation conductance (G). Per-unit-length resistance and inductance of an actual transmission line are time and frequency dependent. The current $I(t, x)$ in the transmission lines after the loop has been switched off obeys the equation (Kozhevnikov 2006, 2009):

$$\frac{\partial^2 I}{\partial t^2} - \frac{1}{LC}\frac{\partial^2 I}{\partial x^2} + \frac{1}{L}\int_0^t R(\tau)\frac{\partial I(t-\tau)}{\partial t}d\tau = 0. \tag{8}$$
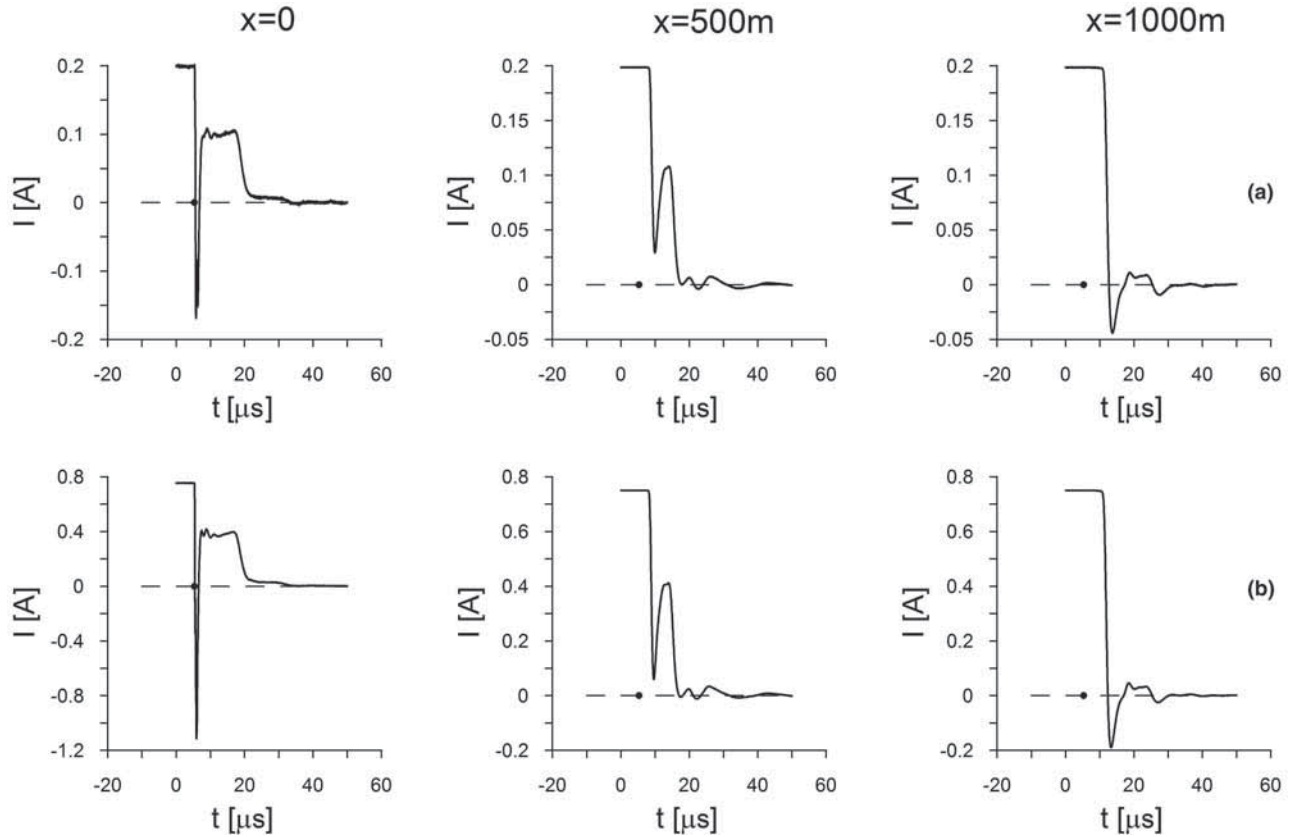
Figure 7 Switch-off waveforms of 0.2 A (a) and 0.75 A (b) currents at different points of the 500 m by 500 m loop perimeter.

Solving (8) is a tough problem in a general case. However, even presentation of the loop as a combination of two lossless, or 'ideal' transmission lines the parameters of which do not depend on the time or frequency clearly illustrates the difference between turning off low and high currents. For a lossless transmission line, equation (8) reduces to the simple wave equation:

$$\frac{\partial^2 I}{\partial t^2} - \frac{1}{LC}\frac{\partial^2 I}{\partial x^2} = 0. \tag{9}$$
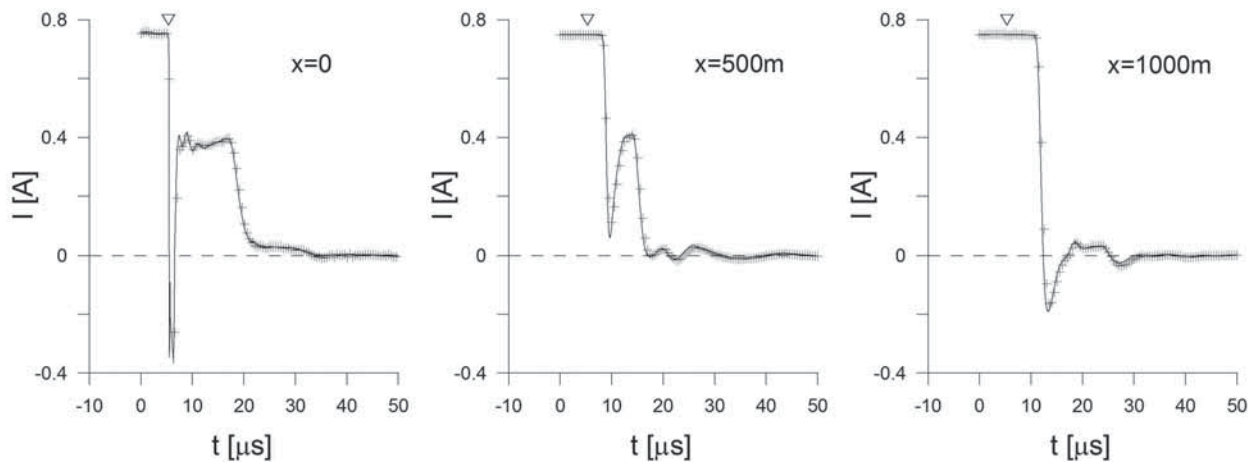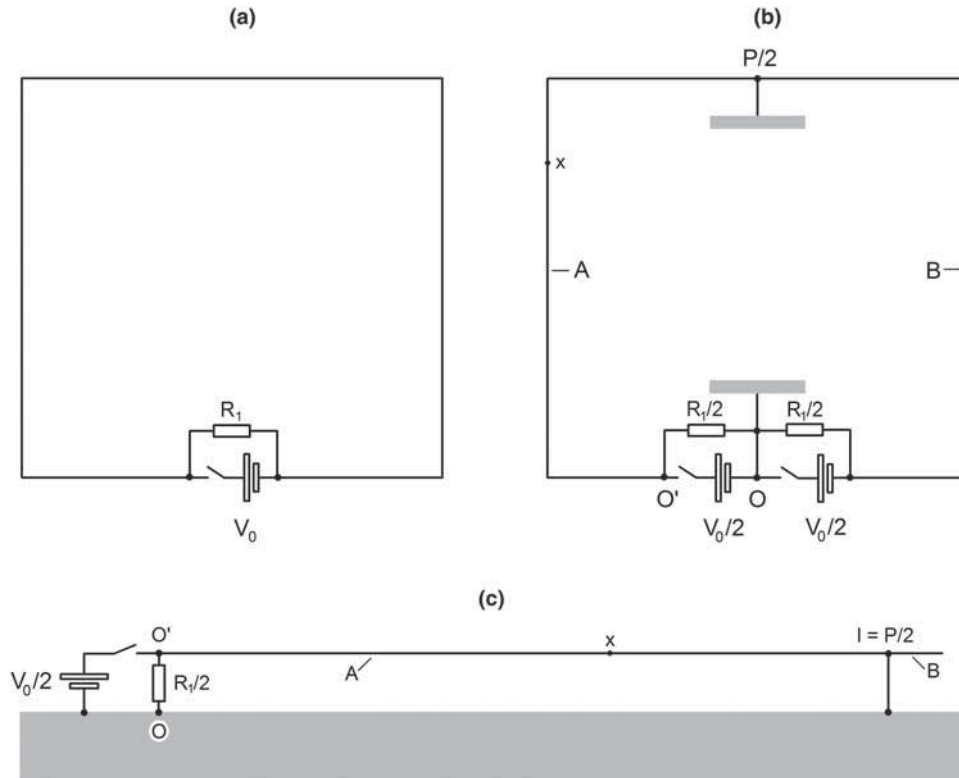

Figure 8 Turn-off waveforms of the 0.2 A (small crosses) and 0.75 A (solid line) currents. When plotting graphs for 0.2 A current, current's values were multiplied by 3.75. An inverted triangle marks the instant of time when the transmitter disconnects the loop from the battery.

Figure 9 Transmitter loop, battery, switch and matching resistor R_1 (a); same loop, battery and matching resistor presented as two identical transmission lines A and B, two batteries and two resistors (b); line A grounded at the output.

An illustrative picture of turning off the current is given by solving equation (9) using a technique that allows one to 'see' how the current in an ideal loop is switching off at various points of the loop perimeter after disconnecting the battery from the loop's terminals (Peterson, Gregory, and Durgin 2009; Kozhevnikov 2009, 2016). This technique is used to present the current switching off as a superposition of current waves travelling in opposite directions along transmission lines formed by the loop wire and the ground.

First consider switching off the steady current I_0 in a non-shunted ($R_1 = \infty$) loop. When the switch disconnects the loop from the battery, at the input of each line there appears a step-like current wave. In the case being considered ($R_1 = \infty$), the direction, or polarity, of the current forming the step-like wave is opposite to that of the steady current which was flowing in the loop before the switch has been opened, and the amplitude of this negative current step is equal to I_0 (Fig. 10a).

The waves are travelling to the point $x = P/2$. When they reach this point, which has zero potential and therefore can be considered as grounded, the reflected waves arise here that are travelling back to the loop's terminals. Thus, the to-tal current in each line is the sum of the steady current and the two current waves: the first wave is travelling from the terminal towards the central point of the loop perimeter, the second wave—from this point back to the terminal. When the reflected waves reach loop terminals, they are again reflected, since the transmission line is open at $x = 0$ and $x = P$ (R_1 in Fig. 9a and, therefore, $R_1/2$ in Figs 9b and 9c are equal to infinity). From this point on, the current distribution along each of the lines is the sum of three travelling waves and the steady-state current. Later, new reflections occur, and the superposition of waves travelling in both directions manifests itself as a standing wave with period T. In a lossless line, this process would continue perpetually.

The 'snapshots' of the current distribution $I(x)$ along the perimeter of a lossless loop at fixed times (Fig. 10a) and $I(t)$ waveforms at fixed points of the loop perimeter (Fig. 10b) indicate that the closer the observation point is to the centre of the loop perimeter, the more the current turn-off retards (relative to the instant at which the switch disconnects the loop from the battery). The current distribution along the loop is symmetrical about the Y-axis; however, there is no symmetry with respect to the X-axis. Therefore, if the loop is located on
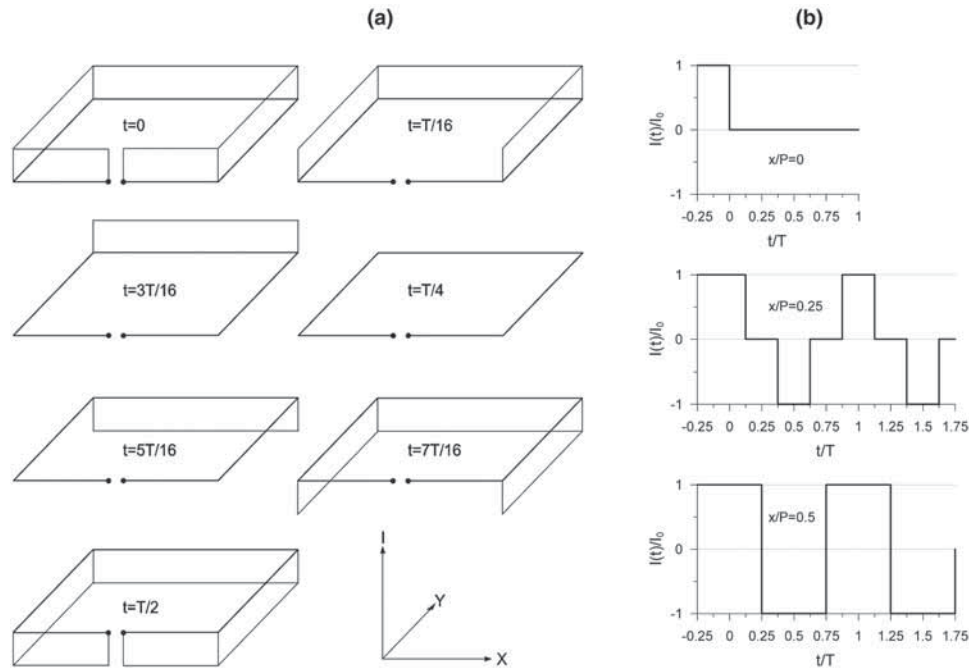
Figure 10 Current turn-off in an ideal (lossless) non-shunted ($R_1 = \infty$) loop (free oscillation mode). (a) Snapshots of the current distribution along the loop perimeter. (b) Current versus time plots for some points of the loop perimeter. At $t = 0$, the loop is disconnected from the battery. T is period of the current free oscillations.

the surface of an electrically asymmetrical ground, the early-time transient electromagnetic (TEM) response will depend on the location of the loop terminals.

Now consider the loop shunted by a matching resistor with the resistance R_1 equal to twice the high-frequency characteristic impedance Z of the transmission lines. In this case, current waves travelling from the central point of the loop perimeter to the loop's input do not reflect, and the current turn-off terminates. Field measurements have shown that for wires commonly used in TEM surveys, R_1 is in the range 350–500 ohms (Kozhevnikov and Nikiforov 1998; Kozhevnikov and Nikiforov 2000; Helwig and Kozhevnikov 2003; Kozhevnikov 2006, 2009; Kozhevnikov and Helwig 2014).

Figure 11(a) shows snapshots of the current distribution along the perimeter of a lossless loop at various times after disconnecting the loop from the battery. The loop is shunted by a matching resistor R_1 (not shown in the figure). Figure 11(b) indicates that the current turn-off waveforms differ depending on the position of the observation point on the loop perimeter. According to Fig. 11, in the case being considered (lossless matched loop), the total time during which the current is turned off is equal to the half-period ($T/2$) of the current's free oscillations.

In Fig. 12, experimental graphs of the 0.75 A current turn-off (see Figs 7 and 8) are shown together with those calculated using the presentation of the loop as a combination of two lossless transmission lines (see Fig. 9). The modelled current turn-off waveforms of Fig. 12 are calculated for $T = 25$ μs, a value providing the best fit between the experimental and model data. The period of the natural current oscillations in the non-shunted ($R_1 = \infty$) loop, as found by direct measurement, is 27.2 μs.

As Fig. 12 indicates, presentation of a loop as a combination of two lossless transmission lines accounts for the main features of the low current turn-off. In details, the current turn-offs in actual and ideal loops differ. Due to the frequency dispersion of an actual loop's parameters, the current turn-off waveforms are smoothed compared with those for a lossless loop. Near the loop terminals, there is a short current pulse of negative polarity. These 'second-order' phenomena were discussed earlier (Kozhevnikov and Helwig 2014; Kozhevnikov 2016), and are not considered in this article.

6 DISCUSSION

As shown above, due to symmetry, the loop can be represented as a symmetrical combination of two transmission lines. In
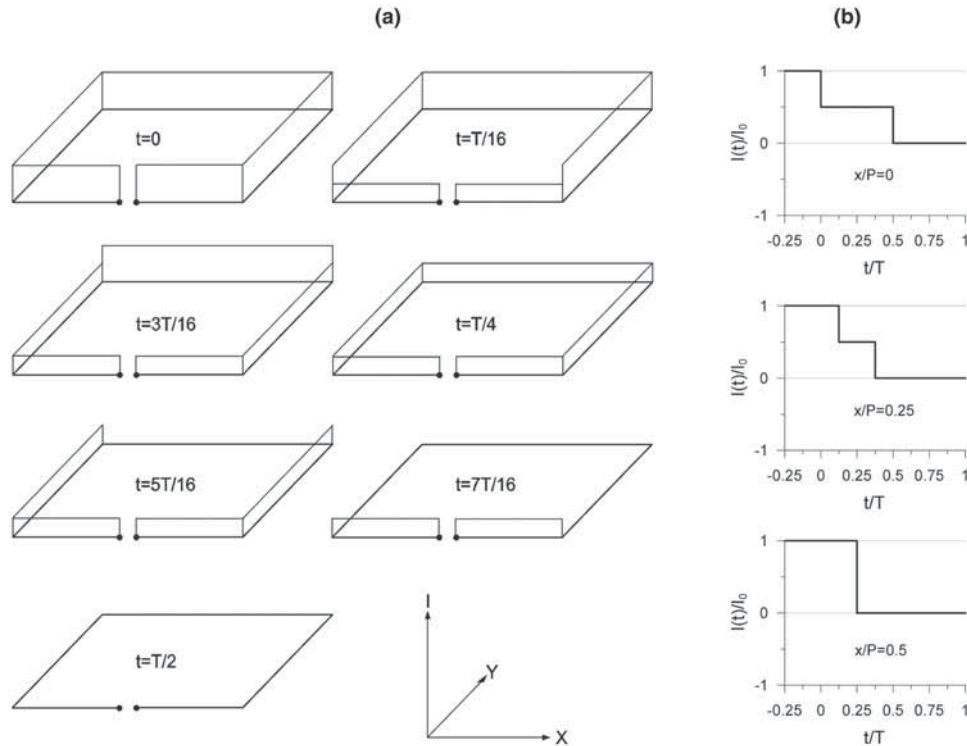
Figure 11 Switching off the current in a lossless loop shunted by a resistor with resistance equal to twice the characteristic impedance of transmission line (matching mode). (a) Current's distribution along the loop perimeter for fixed points in time. (b) Current's turn-off waveforms at various points of the loop perimeter.

principle, the transmission lines theory can explain the shutdown of an arbitrary current in the transmitter loop. However, since the resistance of the TVS is extremely nonlinear, finding the solution for an arbitrary current is a difficult task (Peterson, Gregory, and Durgin 2009). Therefore, we limited

ourselves to considering two cases, namely, turning off low and high currents.

When the current being switched off is low, the voltage across the loop terminals does not exceed the TVS clamping voltage. In this case, the TVS resistance is much
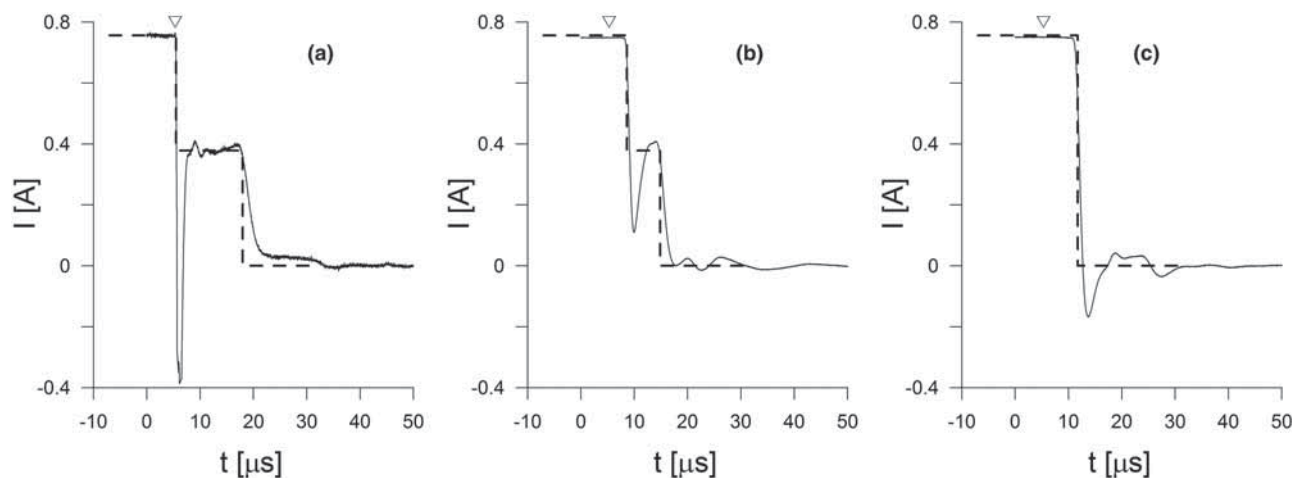
Figure 12 Measured (solid line) and modelled (dashed line) turn-off waveforms of 0.75 A current at various points of the 500 m by 500 m loop perimeter. The inverted triangle marks the instant of time when the transmitter disconnects the loop from the battery.

higher than the characteristic impedance of transmission lines, and current turn- off can be represented as the sum of stepwise current waves travelling along the lines in both directions.

When the current being switched off is high, the dynamic resistance of the TVS is much less than the characteristic impedance of the transmission line. In this case, the loop behaves as an equivalent lumped circuit, and the current decay is described by an ordinary differential equation (3).

Note that, in principle, presentation of a loop as a combination of two transmission lines can explain switching off both low and high currents. As for the equivalent lumped-circuit model, it correctly predicts turning off the high current, but is not able to explain turning off the low one.

Since the solution of the wave equation with account for all details of turning off the transmitter current is hardly possible, at the moment we only briefly comment on these details.

According to Figs 5(a), 11 and 12, turning off a high current in a 500 m by 500 m loop can be represented by the solution of wave equation (9) as a superposition of travelling step-current waves. The decay of a high current (see Fig. 5a) as a whole occurs linearly, and only at the earliest times is complicated by the same wave phenomena that constitute the low current turn-off. These wave effects are seen also in the earliest portion of the high current turn-off for a 300 m by 300 m loop (see Fig. 2).

When commenting on a short undershoot of the current after the linear shutdown, which is similar to that shown in Fig. 2, Wang *et al.* (2016) explain it as a combination of TVS and transmitter loop responses at the final stage of current turn-off. The authors present a detailed simulation of linear current shutdown, but do not provide the corresponding equations with which it would be possible to calculate the current undershoot.

Along with large, flexible, single-turn transmitter loops, small multi-turn loops are also widely used in transient electromagnetic (TEM) surveys. Since the inductance of a multi-turn loop is proportional to the square of the number of loops' turns (Grover 1973), a large current in such a loop is turned off slowly. Suppose that instead of a single-turn square loop with the side length A, one wants to use a multi-turn square loop with a side length a, and $a = A/n$, where n is an integer. Suppose also that the magnetic moment of the multi-turn loop and current in it should be the same as those of a single-turn loop. Obviously, both loops must have the same effective area, whence it follows that the number of turns N, forming a small loop, is equal to n^2.

It is straightforward to show that the inductance of such a multi-turn loop is n^3 times larger than of a single-turn loop with the same magnetic moment. Accordingly, the duration of the current turn-off in a small multi-turn loop will be n^3 times longer than in a large single-turn loop. Because of this, the multi-turn loop is not suitable as a source of the primary magnetic field in the near-surface TEM studies.

7 CONCLUDING REMARKS

As shown by the field measurements and simulation results, the high and low currents in a transmitter loop are turned off in fundamentally different ways.

During turning off the low current, the voltage surge across the loop does not exceed the clamping voltage V_c. In this case, the transmitter loop manifests itself as distributed network that can be represented as a symmetric combination of two transmission lines grounded at the central point of the loop's perimeter. This presentation of the loop allows, using the transmission lines theory, to calculate the current at any point of the loop perimeter for any instant of time.

If the voltage surge is lower than V_c, the turn-off waveform and duration do not depend on the current's magnitude. In this case, the duration of the current turn-off is determined by the period of natural current oscillations and of the resistance of a shunting resistor. To suppress natural current and voltage oscillations optimally, the resistance of a matching resistor has to be equal to twice the characteristic impedance of a transmission line formed by the loop wire and the underlying ground. For an ideal (lossless) loop, the turn-off time is equal to half the period of the loop's natural oscillations. An actual loop consists of lossy transmission lines the parameters of which depend on frequency/time; because of this, the total time of the current turn-off is usually somewhat above $T/2$ (Kozhevnikov 2016).

In principle, the low current can be turned off even faster. If one connects the matching resistor in series with the loop wire in the middle of the loop perimeter, step-like current waves travelling to this point from the loop terminals will not reflect here, and the current shutdown will end at time $t = T/4$. It is the shortest possible duration of the transmitter current's turn-off.

If the current being turned off is low, the early-time primary magnetic field (due to the retardation effects) differs from that assumed by the conventional theory of the transient electromagnetic (TEM) method.

As for the high current, it is such that during its shutdown the voltage surge across the loop would exceed the clamping

voltage V_c if it were not limited by means of a clamping circuit. In this case, the current is switched off synchronously and linearly with time at any point of the loop perimeter. The wave phenomena manifest themselves only at the beginning of the current's shutdown for a time that is much less than the total turn-off time. The measured waveform and duration of the high current turn-off are in good agreement with those predicted by an equivalent lumped-circuit model.

In our opinion, there are two reasons why the article may be of interest to those engaged in the theory and/or practice of electromagnetic prospection methods. First, it contributes to a general understanding of how the current in the transmitter loop is turned off. Second, the article shows how the parameters of a transmitter loop determine the current turn-off duration and, thus, the minimum depth of the TEM sounding method.

DATA AVAILABILITY STATEMENT

Data are available on request from the authors.

CONFLICTS OF INTEREST

The authors declare that there is no conflict of interest.

ORCID

Nikolai O. Kozhevnikov (ID)
https://orcid.org/0000-0003-1664-6706

REFERENCES

Asten M.W. 1987. Full transmitter waveform transient electromagnetic modeling and inversion for soundings over coal measures. *Geophysics* **52**, 279–288.

Christiansen A.V., Auken E. and Viezzoli A. 2011. Quantification of modeling errors in airborne TEM caused by inaccurate system description. *Geophysics* **76**, F43–F52.

Ferreira J.A., Kane I.J., Klinkert P.h. and Hage T.B. 2004. A square-wave current inverter for aircraft-mounted electromagnetic surveying systems. *IEEE Transactions on Industry Applications* **40**, 2013–2019.

Fitterman D.V. and Anderson W.L. 1987. Effect of transmitter turn-off time on transient soundings. *Geoexploration* **24**, 131–146.

Fu Z.h., Zhou L. and Tai H.-M. 2007. Current pulse generation for transient electromagnetic applications. *Electric Power Components and Systems* **35**, 1201–1218.

Grover F.W. 1973. *Inductance Calculations (Working Formulas and Tables)*. Instrument Society of America, New York.

Helwig S.L. and Kozhevnikov N.O. 2003. Schwingungen in TEM Sendesignalen zu frühen Zeiten. *20 Kolloquium Elektromagnetische Tiefenforschung, Königstein, 29.09.-3.10.2003, Hrsg.: A. Hördt und J.B. Stoll*, 11–20.

Kozhevnikov N.O. 2006. An ungrounded horizontal loop as a system with distributed parameters. *Geofizika* No. 1, 29–39. (in Russian).

Kozhevnikov N.O. 2009. Applying the transmission line theory to study ungrounded horizontal loop self-transients. *Russian Geology and Geophysics* **50**, 222–233.

Kozhevnikov N.O. 2016. Current turn-off in an ungrounded horizontal loop: experiment and theory. *Russian Geology and Geophysics* **57**, 498–505.

Kozhevnikov N. and Helwig S. 2014. Very early time response of an ungrounded horizontal loop: theory and experiment. *Extended Abstracts, 22nd EM Induction Workshop Weimar, Germany*.

Kozhevnikov N.O. and Nikiforov S.P. 1998. Distributed EM parameters of an ungrounded horizontal loop and their relation to the near-surface geoelectrical features. *Proceedings of the Symposium on the Application of Geophysics to Engineering and Environmental Problems*, Chicago, USA, EEGS, 1019–1027.

Kozhevnikov N.O. and Nikiforov S.P. 2000. Early time TEM response of an ungrounded horizontal loop – a new look. *62nd EAGE Conference, Expanded Abstracts*, Glasgow, D-11.

Liu L., Qiao L., Liu L., Geng Z.h., Shi Z. and Fang G. 2019. Applying stray inductance model to study turn-off current in multi-turn loop of shallow transient electromagnetic systems. *IEEE Transactions on Power Electronics* **35**, 1711–1720.

Ott H.W. 2009. *Electromagnetic Compatibility Engineering*. John Wiley & Sons, Inc., New Jersey.

Peterson A.F., Gregory D. and Durgin G.D. 2009. *Transient Signals on Transmission Lines: An Introduction to Non-Ideal Effects and Signal Integrity Issues in Electrical Systems*. Morgan and Claypool Publishers.

Raiche A.P. 1984. The effect of ramp function turn-off on the TEM response of layered earth. *Exploration Geophysics* **15**, 37–41.

Schamper C., Auken E. and Sørensen K. 2014. Coil response inversion for very early time modelling of helicopter-borne time-domain electromagnetic data and mapping of near-surface geological layers. *Geophysical Prospecting* **62**, 658–674.

Sharlov M.V., Buddo I.V., Misyurkeeva N.V., Shelokhov I.A. and Agafonov Y.u.A. 2017a. Transient electromagnetic surveys for high-resolution near-surface exploration: basics and case studies. *First Break* **35**, 63–71.

Sharlov M.V., Kozhevnikov N.O. and Sharlov R.V. 2017b. Lake Baikal – a unique site for testing and calibration of near-surface TEM systems. *Near Surface Geoscience*, Malmö, Sweden.

Sokolov V.P., Tabarovsky L.A. and Rabinovich B.I. 1978. Transformation of TEM responses measured with current pulses of non-ideal waveforms. In: *Electromagnetic Fields in Exploration Geophysics: Theory and Practice* (ed. V.P. Sokolov), pp. 81–92. IGG SO RAN, Novosibirsk (in Russian).

Sternberg B.K., Dvorak S.L. and Feng W. 2017. Design and verification of large-moment transmitter loops for geophysical applications. *Journal of Applied Geophysics* **136**, 211–218.

Vishnyakov A.E. and Vishnyakova K.A. 1974. *Excitation and Measurement of Electromagnetic Fields in EM Exploration.* Nedra, Leningrad. (in Russian).

Wang S.h., Yin C.h., Lin J., Yang Y. and Hu X. 2016. Bipolar square-wave current source for transient electromagnetic systems based on constant shutdown time. *Review of Scientific Instruments* **87**, 034707.

Zakharkin A.K. 1981. *TEM Surveys with TZIKL Instrument: Methodological Guide.* SNIIGGiMS, Novosibirsk. (in Russian).

Zhang L., Duan Q., Sun H., Huang T., Shi1 J., Wu D. *et al.* 2014. Design of transient electromagnetic transmitter based on FPGA. *Applied Mechanics and Materials* **496–500**, 630–633.

Zhao H., Liu L., Wu K., Qi Y. and Fang G. 2013. Constant voltage-clamping bipolar pulse current source for transient electromagnetic system. *Electric Power Components and Systems* **41**, 960–971.